

Menangle Underbridge Assessment
Appendix D
Cleat Tests

Menangle Underbridge Assessment

Appendix D

Cleat Tests

Table of Contents

1.	Objective	3
2.	Test piece	3
3.	Design of fatigue test	3
4.	Calibration.....	5
5.	Cyclic test program	6
6.	Ultimate strength test	7
7.	Acoustic Emission monitoring.....	8
8.	Acoustic Emission evaluation.....	8
9.	Examination of fracture surfaces	8
10.	Fatigue assessment.....	9
11.	Conclusions.....	12

CLEAT TESTS

1. Objective

In this Appendix a fatigue test is conducted on part of an angle cleat taken from the bridge and subjected to cyclic bending to simulate the cycles which occur in practice. The objective is to establish whether fatigue crack growth is occurring or whether it can occur in the future from existing cracks. Acoustic Emission is used to monitor fatigue crack growth.

The fracture surface of the cracked cleat, the testing of which is described in this Appendix, has been discussed extensively in Appendix A. There it was concluded that the pre-existing crack was old and that there was no evidence of fatigue cracking at all.

This Appendix provides the quantitative assessment of fatigue strength in this cracked cleat. Since the pre-existing crack is typical for the cleats which have cracks it is concluded that the findings for this crack can be extended to the rest of the cleats.

2. Test piece

The bottom part of the cleat removed from the structure was cut off as shown in figure C1, Appendix C, and prepared for testing. This piece was 135 mm wide. It contained the crack shown in Appendix A (Figures A2 and A3). It also contained the bottom edge, which on the cross girder leg was bevelled to assist fit-up. The edge was of indifferent quality, as indicated by Figures A4 – A6.

The test piece contained rivet holes, one close to the crack tip. The crack had actually reached past this hole. Rivet holes were intersected by the saw cut of the upper edge of the test piece. These holes and excisions would amplify stresses in critical regions, if they had any effect at all, and therefore did not detract from the fatigue assessment.

The plate thickness varied at the fillet, but was mostly 13 mm. The angle cleats were apparently formed with an inner radius of 12.7 mm (half inch) and an outer radius of 25.4 mm (one inch).

3. Design of fatigue test

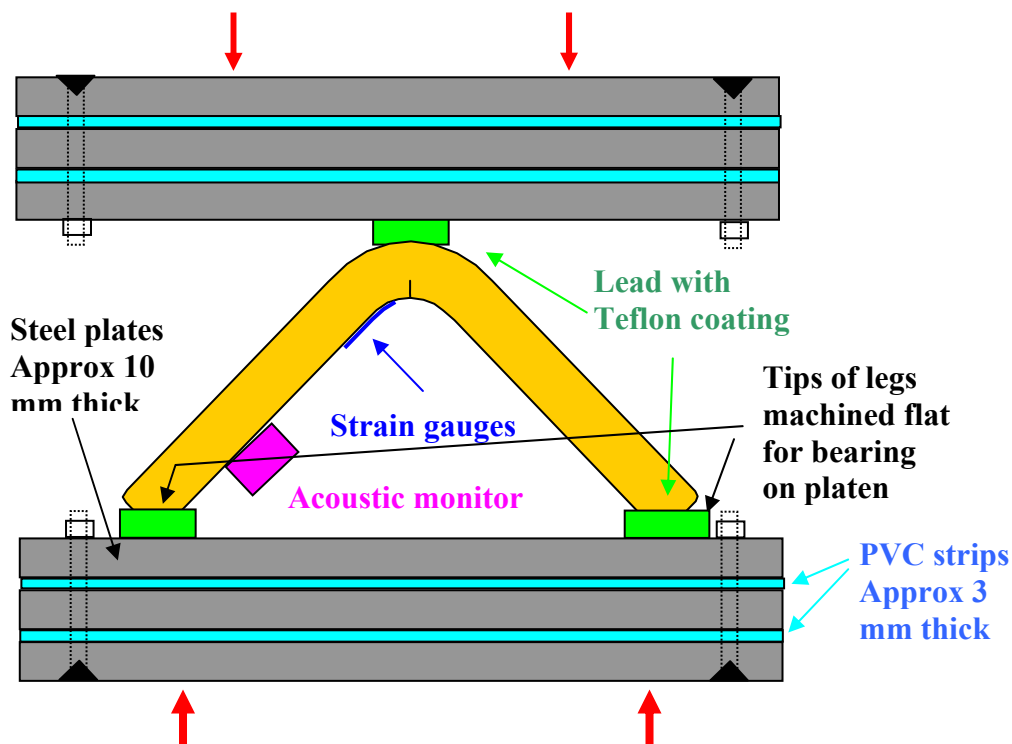


Figure D1 – Test setup schematic

The highest stresses in the cleats measured on Cross Girders S1-CG26 and S1-CG27 were at location I, north side of CG27, down track. This strain gauge was on the edge of the fillet, about 12 mm above the bottom edge, on the box girder face. Using a Modulus of Elasticity of 187 GPa the stress at this strain gauge over all the test runs ranged from -35.8 MPa (compression) to + 23.5 MPa (tension). The strain gauge at location I on the south side of S1-CG27 recorded about two thirds of the range of the north side. Other strain gauges recorded even less.

The stress regime at the fillet is considered to be primarily one of flexure, with added membrane stresses in the direction of the cross girder. It is very complex, especially due to the variable clamping and close proximity of the rivets. The stresses of this ‘worst case’ will be taken as an estimate of maximum likely effects to be experienced in practice. Discretionary factors can be added for impact, since the filed measurements were made at 40 kph or less speed.

In the laboratory the field stresses were approximated through a three-point bending test, as shown in Figure D1. Since effective acoustic emission monitoring requires acoustic isolation of the test piece some effort went into blocking the path of noise from the testing machine. Lead was used to distributed the contact pressure from the platen evenly over the heel of the angle, where there were surface irregularities.

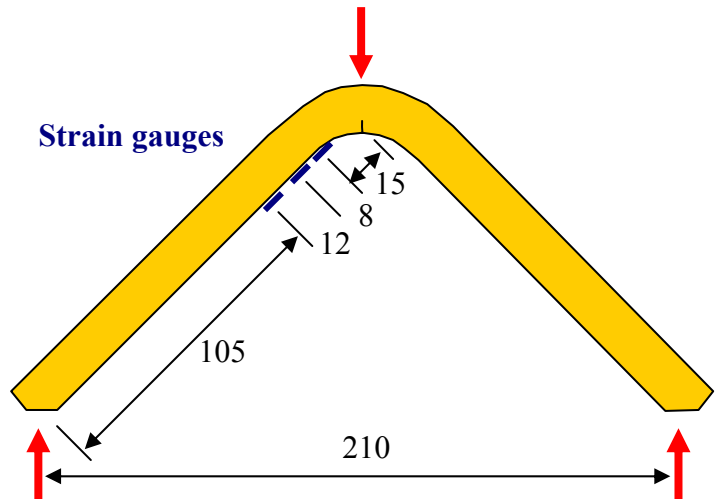


Figure D2 – Strain gauge locations

Three strain gauges were attached to monitor the gradient of strain up to the fillet. The strain gauges were in line with the tip of the crack revealed by magnetic particle inspection. The curved surface of the fillet was considered unsuitable attaching strain gauges, and close proximity to the crack tip should be avoided. Critical dimensions for the estimation of stresses are shown in Figure D2, and the set-up in the testing machine is shown in Figure D3.

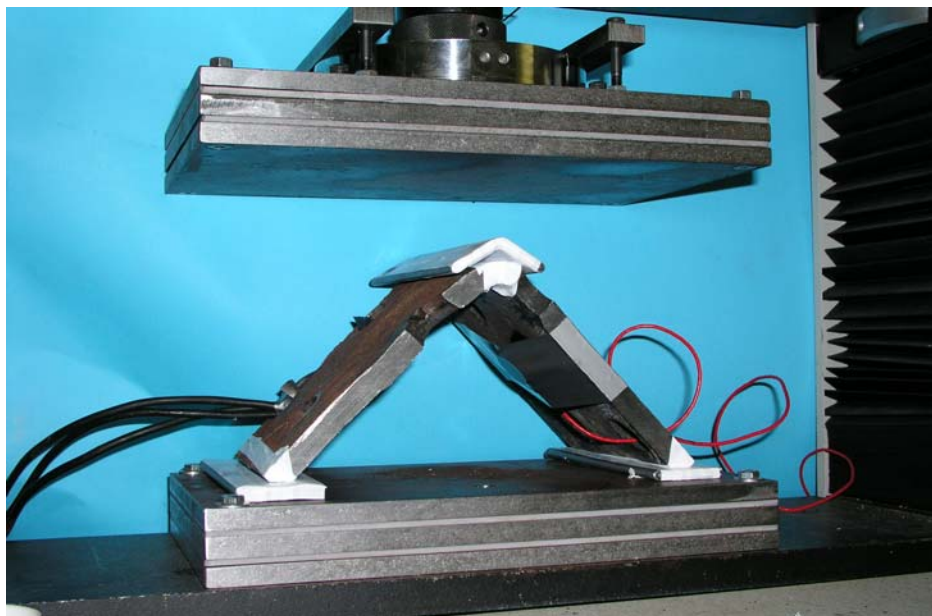


Figure D3 – Cleat segment ready for testing (photo ATTAR)

4. Calibration

A static test was carried out to settle the test piece in place and to compare measured strains with predictions. The specimen was loaded under displacement control up to 9.65 kN, where it was held in position control for a few minutes before unloading. Figure D4 shows the strain versus load history.

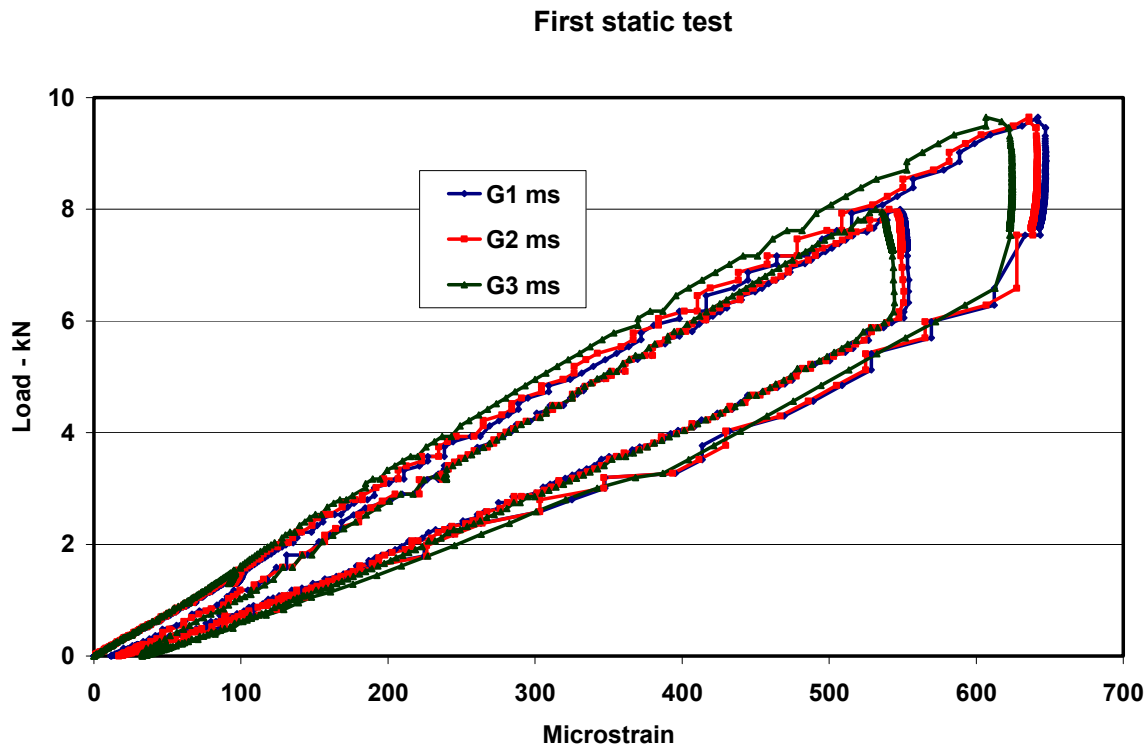


Figure D4 – First $\sigma\epsilon$ test, strains versus load

A striking feature of this test was the relaxation in the stresses which occurred when the cleat was held in position under load. The load falls steadily, but the strains return to zero when the specimen is unloaded. This phenomenon was observed in the cyclic load tests. On reloading the same loading path is followed.

The relaxation is attributed to the lamellar characteristics of wrought iron. Shear transfer in the build up of bending moment relies on friction and interlock of asperities of adjacent laminations. (A lot of the acoustic emission detected is attributed to this.)

In Table D1 a comparison is made between measured strain and predicted strains of the three strain gauges under a load of 8.0 kN. A Modulus of Elasticity of 187 GPa was assumed. Allowance was made for the axial component of stress along the inclined slope of the leg. The cross-section of the leg was taken to be 135 mm wide x 12.7 mm thick.

Table D1 – Comparison of measured with predicted strains at 8.0 kN load.

Strain Gauge	Estimated Stress	Estimated Strain	Measured Strain
G1	102.0 MPa	545 μs	541 μs
G2	95.6 MPa	511 μs	519 μs
G3	85.4 MPa	457 μs	496 μs

There is good agreement between estimated and measured strains, especially for G1 and G2. There are many uncertainties due to the presence of rivet holes and cracks.

Extrapolating linearly to the root of the fillet the best estimate of peak strain at the crack, without allowance for stress concentration effects, is 78 microstrain per kilonewton (78 $\mu\text{s/kN}$), with a corresponding stress of 14.6 MPa/kN. This stress is the *nominal stress* used in discussing results.

This stress does not include the amplification due to the plate at the fillet being in a circular arc with an inner radius of 12.7 mm. According to Timoshenko and Goodier, the inside flexural stress is increased 29% over that in a straight bar of the same cross-section, while the outside stress is reduced. Whether this ‘stress concentration’ should be included in the fatigue assessment is not clear.

5. Cyclic test program

Seven blocks of loading were applied as shown in Table D2.

Table D2 – Cyclic loading program applied to angle cleat specimen

Test No	Cyclic Test Load	Nominal stress range	Number of Cycles
1	0.2 to 1.2 kN	14.6 MPa	351
2	0.2 to 2.2 kN	29.2 MPa	359
3	0.2 to 4.2 kN	58.4 MPa	342
4	0.2 to 6.2 kN	87.6 MPa	494
5	0.2 to 8.2 kN	116.8 MPa	553
6	0.2 to 10.2 kN	146.0 MPa	372
7	0.2 to 12.2 kN	175.2 MPa	440



To distinguish between background acoustic emission associated with the test setup and that due to mechanical action within the test piece a replica of the angle cleat test piece was made out of mild steel cut from a square hollow section. It had the same geometric shape. The replica was free of surface defects and cracks (see Figure D5).

An acoustic emission monitor was attached to this specimen and it was subjected to a cyclic loading similar in range to the test cleat. The cyclic loading program is shown in Table D3.

Figure D5 – Test piece replica in mild steel

Table D3 – Cyclic load program applied to mild steel replica

Test No	Cyclic Test Load	Nominal stress range	Number of Cycles
2	0.2 to 2.2 kN	29.2 MPa	40
4	0.2 to 6.2 kN	87.6 MPa	80
5	0.2 to 8.2 kN	116.8 MPa	100
6	0.2 to 10.2 kN	146.0 MPa	150
7	0.2 to 12.2 kN	175.2 MPa	260

The AE monitoring and assessment of the tests is discussed in sections 7 and 8 below.

6. Ultimate strength test

After completion of the cyclic loading tests the test piece was loaded to collapse, finally being squashed flat between the platens of the testing machine. This broke the specimen open at the fillet, exposing the original crack for microscopic examination. Figure D6 depicts the load versus the ram displacement of the testing machine. Figure D7 depicts the load versus strain relationship.

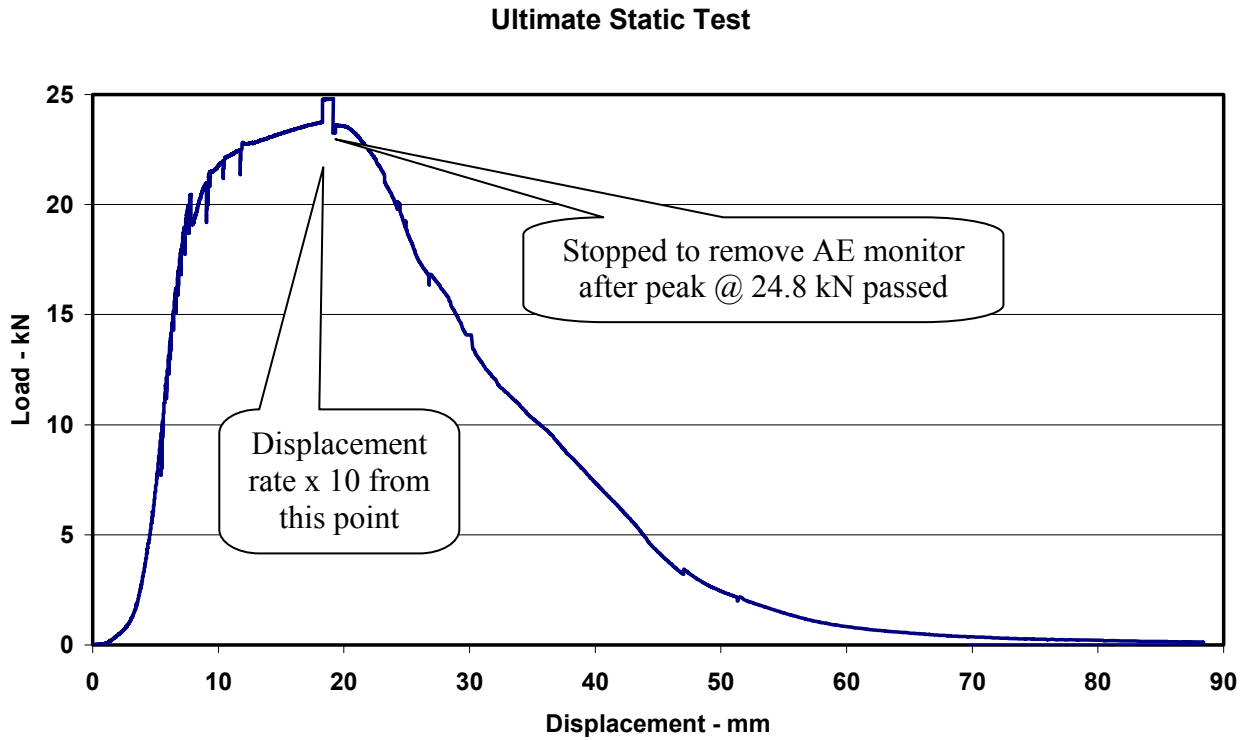


Figure D6 – Ultimate strength test – load versus ram displacement

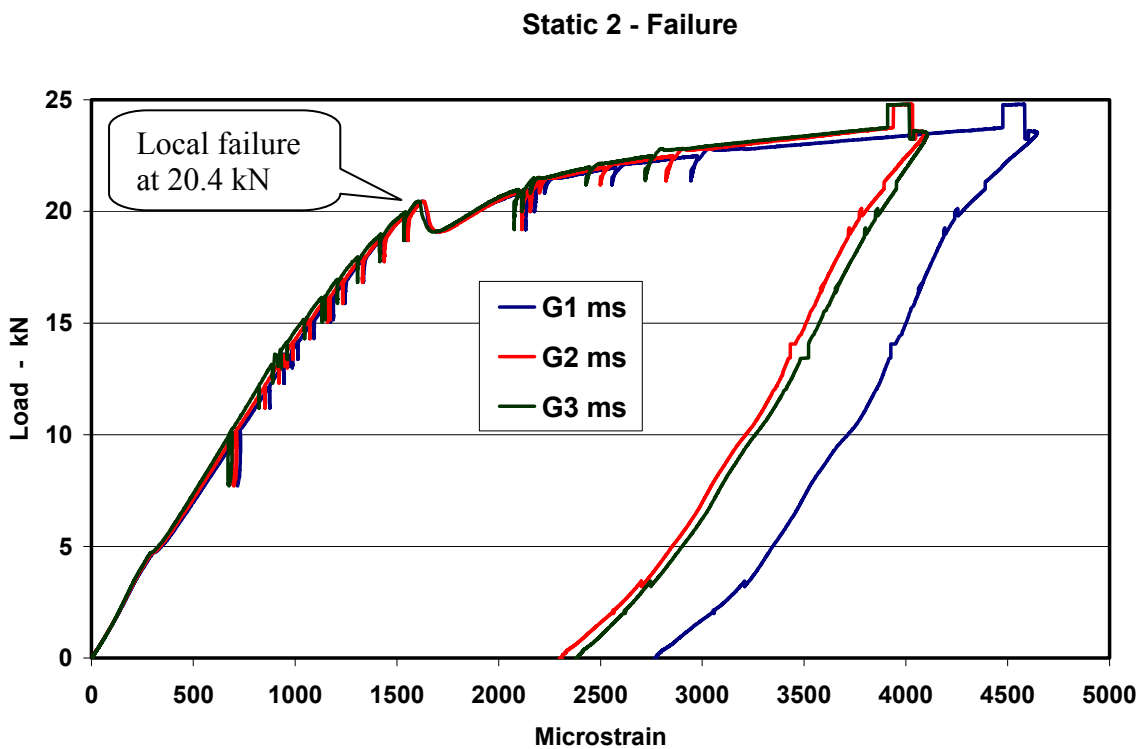


Figure D7 – Ultimate strength test – load versus strains

During this test the ram displacement was stopped about 18 times for a minute or two to allow creep to take place. This is evident in the strain and displacement graphs of Figures D6 and D7. It is believed that slip on the interface between laminations of the metal contributed to the relaxation in strain, which has the effect of postponing the onset of yielding in the outer laminations.

A fracture type of noise was heard when the load reached 20.4 kN, and the load fell back to 19.1 kN on the resumption of ram movement, after which the load continued to rise with further displacement. It is assumed that a local failure of one of the laminations occurred.

When the load reached about 23.5 kN and was increasing very slowly the ram velocity was increased sharply to speed up the test. The load increased sharply and shortly afterwards peaked and unloading occurred as the material failure slowly propagated inwards from the outer layers. The strain gauges, being outside the failure zone, unloaded at this time.

The ultimate load attained was 24.8 kN. If elastic-perfectly plastic material behaviour is assumed the corresponding 'yield' stress is 239 MPa. This value is much higher than 187 MPa 'Nominal Yield Stress' based upon stress at 1000 microstrain, reported in Appendix C. The result is not surprising, as the wrought iron stress-strain relationship has a transition from yield to strain hardening without a yield plateau as observed in mild steel.

7. Acoustic Emission monitoring

Details of the AE monitoring are contained in ATTAR Test Report No. 03/5740. The results reported include the amplitude and duration of the 'hits', the cycle no. and the load level within the cycle at which the hits occurred.

8. Acoustic Emission evaluation

Full evaluation of the AE monitoring is contained in ATTAR Test Report No. 03/5740. ATTAR made the following assessment, which is endorsed by Grundy Consultancy:

"The acoustic emission monitored during the cyclic tests appeared not to be due to any fatigue crack growth, rather, it would probably have come from the following sources:

- Crushing of the rusted and flaky surface between the existing crack under load.
- Rubbing of the existing crack surface faces.
- Elastic and plastic deformation of the material.
- Movement between laminated surfaces in the wrought iron.
- Movement or rubbing of the contact surfaces of the test angle."

ATTAR state further:

"None of the acoustic emission detected during the fatigue testing was indicative of crack growth. Most acoustic emission detected during testing came from the crushing of an oxide layer and the rubbing of the existing fracture surface. No fatigue crack growth occurred during the test."

9. Examination of fracture surfaces

The fracture surface has been fully discussed in Appendix A – Assessment of Damage. The ATTAR Test Report added the following comment:

"Examination of the fracture surface under a stereo microscope at magnifications up to 90%, did not show any signs of recent fatigue crack growth, The fracture was typical of a ductile overload failure."

These remarks are in agreement with those made in Appendix A. There was no physical evidence of past fatigue crack growth or of fatigue crack growth during the laboratory testing.

10. Fatigue assessment

General principles

The methodology of fatigue assessment used herein uses the *Detail Classification (or Category)* method. In this method stress concentration effects are included in design curve, which has been determined from laboratory tests. A family of S-N curves are developed. The basic S-N curve relating the number of cycles to failure is shown in Figure D8.

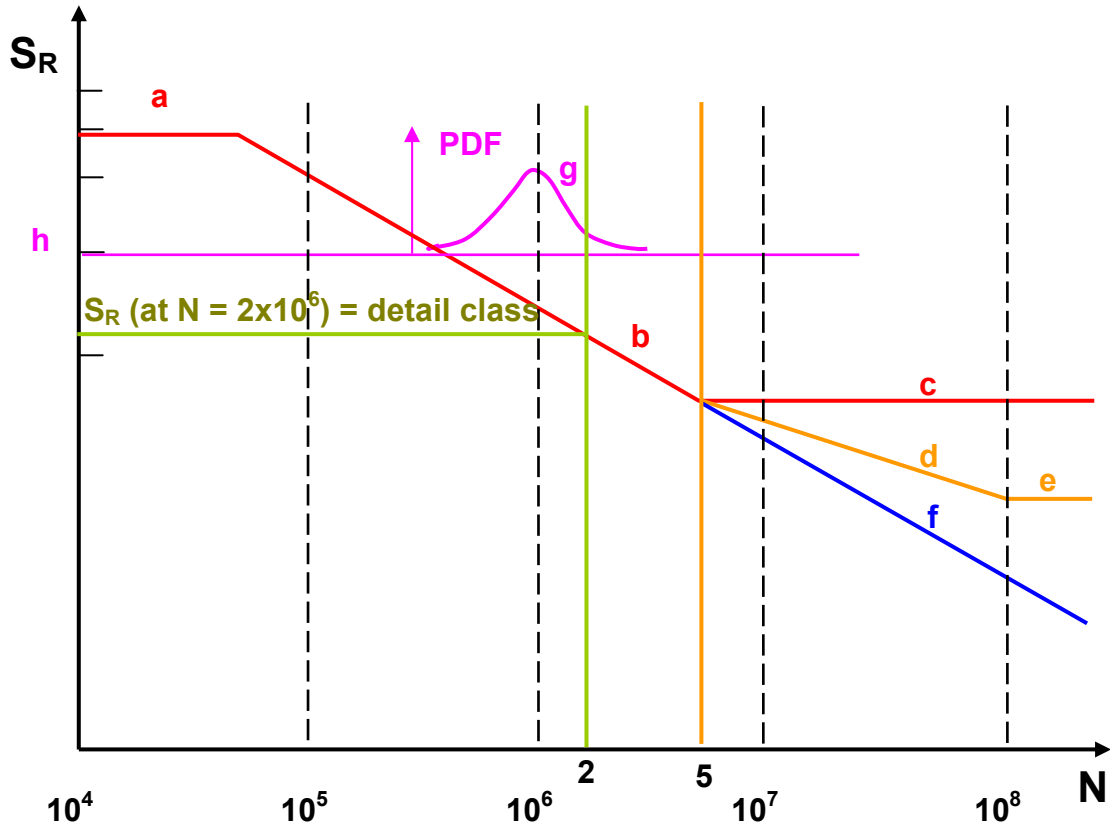


Figure D8 – Basic Fatigue Strength Curve Features

- log-log graph
- S is STRESS RANGE: mean stress is ignored, not relevant
- N is no. cycles to failure at constant amplitude S
- Upper limit to S (usually 1.5 x yield stress) – *line a*
- Constant amplitude fatigue limit (at $N = 5 \times 10^6$, except BS5400: $N = 10^7$) – *line c*
- $N = K S^{-m}$ when $S >$ constant amplitude fatigue limit – *line b*
- $N = K' S^{-(m+2)}$ when $S <$ constant amplitude fatigue limit – *line d*
- Cut-off limit (at $N = 10^8$) – *line e*
- ALL stress cycles must be included if SOME exceed the constant amplitude fatigue limit
- The value of K depends on the DETAIL CLASS
- NO stress concentration factor is used, simply the ambient stress
- S is based upon the BEST ESTIMATE of stress history (load factor is 1.0)
- K is chosen to give mean minus two standard deviations of N, equivalent to 97.7% probability of survival at the end of the design life, assuming normal distribution and deterministic loading – *curve g at stress range h*
- Conservatively, curve *b* and its extension, curve *f*, can be used for fatigue assessment.
- Independent of yield stress (high strength steel no better)

Under variable amplitude loading Miner’s summation is used to assess damage. The fatigue damage index, D , is given by

$$D = \sum_{\text{all } i} \frac{n_i}{N_i} \quad (\text{D1})$$

where n_i = no. cycles of stress at stress range S_i ,

N_i = no. cycles to failure of stress at stress range S_i .

If D is less than unity the detail has not reached the fatigue limit state. It has not ‘failed’.

Fatigue assessment of girder flanges

Although this Appendix is primarily focussed on the angle cleat tests the fatigue assessment of the riveted girders in bending is reviewed for completeness.

A comprehensive fatigue assessment was performed by URS Corporation in determining ratings for the bridge. In the rating assessment some conservative factors were used in classifying details and determining stress cycles, including a dynamic load increment half that specified for strength (since the requirement is to use a best estimate of service load effects).

In this assessment reference will be made to the measured stresses in the field tests rather than computed stresses, recognising that the Class 81 locomotive used in the tests is the heaviest in service to date. Since the test runs were at 40 kph the dynamic increment for that speed is included in the measured data, but the added increment for a speed of 80 kph is uncertain.

In assessing stresses from strain readings Young’s modulus of Elasticity has been assumed as 205 GPa for the steel members and 187 GPa for the wrought iron members. The maximum measured stress ranges in the cross beams are compared with the Constant Amplitude Fatigue Limit in Table D4.

Table D4 – Maximum stress ranges in cross beams versus Constant Amplitude Fatigue Limit

Cross girder	Material	Max stress	Min stress	Range	CAFL
Primary	Steel	20.5 MPa	-0.6 MPa	21.1 MPa	53 MPa
Secondary	Wrought Iron	26.8 MPa	-1.4 MPa	28.2 MPa	70 MPa

In this Table the beams are taken as Detail Class D, BS5400, part 10 – Fatigue. The higher CAFL for wrought iron is recommended by Brühwiler *et al*¹, following an extensive research program. For fatigue assessment this reference recommends ECCS Class 71, which is the same as AS4100 class 71 and equivalent to AASHTO class D.

Even with the maximum possible allowance for dynamic effects, and minor adjustments for net section stresses there is absolutely no way that fatigue can be an issue with the flanges of the cross girders.

Fatigue assessment of Angle Cleat

The difficulty with the fillet of the angle cleat, which contains the ductile cracks, is to assign a Detail Class. Treating the edge of the plate as equivalent to flame cut, and ignoring the crack already present, the best approximation to a class is Class C (BS5400). The equivalent in ECCS and AS4100 specifications is Detail Class 140. The relevant data for assessment are reported in Table D5, which documents the *mean life* data as well we design life data from BS5400.

¹ Brühwiler E, Smith I F C, and Hirt M A. Fatigue and fracture of riveted bridge members. *ASCE Journal of Structural Engineering*, **116**, 1, Pp 198-214, January 1990.

Table D5 – Constant Amplitude Fatigue Limits for Angle Cleat

Code	CAFL
BS5400 – design (mean minus two standard deviations)	78 MPa
AS4100 Detail Category 140	103 MPa
BS5400 – mean	102 MPa

As mentioned above and in Appendix E, the maximum strains were recorded in location I, angle cleat on the north side of cross girder S1-G27, which was about 15 mm from the fillet. The maximum and minimum stresses from all test runs are recorded in Table D6.

Table D6 – Maximum (tensile) and minimum (compressive) stresses recorded at Location I, CG27

Maximum	23.5 MPa
Minimum	-35.7 MPa
Range	59.2 MPa

Since there is no welding in the vicinity of the fillet it might be argued that the compressive stress component of the range can be ignored, or halved in its effective range. However, the conservative assumption that there is severe residual stress in the restrained joint would place all the stress in the tensile range.

Even with the stress ranges in the fillet 31% higher than measured at Location I they are below the BS5400 design value (at which there is a nominal 2.3% probability of fatigue cracking being initiated). Ten million cycles of this stress range would be required to reach the fatigue limit state. The conclusion is that the stresses in the angle cleats are below the range at which fatigue cracking can even be initiated. When the fact that stress ranges of 175 MPa in the laboratory test did not initiate, let alone propagate, fatigue cracks, the conclusion is made *a fortiori*.

An explanation is required for the absence of fatigue cracking at a stress range of 175 MPa, and equally for the choice of Detail Class C as a fatigue category, in spite of the presence of significant cracks, now known to be ductile. This is due to the fundamental difference between steel and wrought iron in notch effect and stress regimes, as shown in Figure D9.

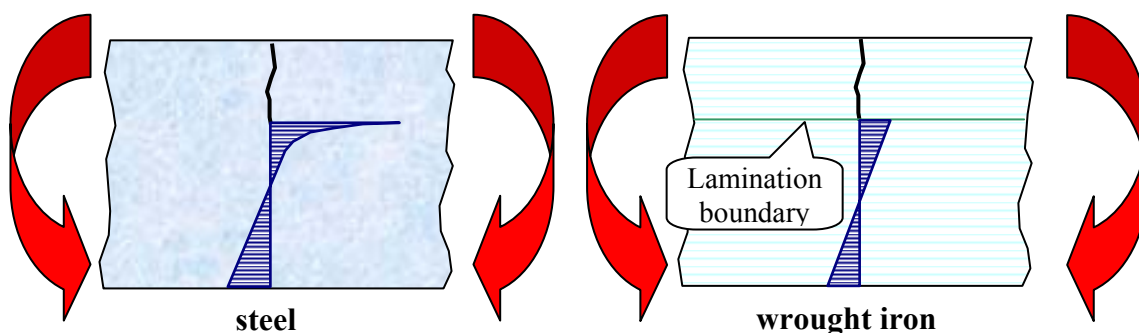


Figure D9 – Stress regimes at cracks in steel and wrought iron plate

A simplified model of fatigue behaviour is proposed. When a crack propagates through an homogeneous steel plate subjected to tensile membrane or bending stress there is a sharp stress concentration at the crack tip, actively driving the crack under cyclic load. The crack in the wrought iron plate encounters a lamination boundary where it stops. A fresh crack has to initiate on what is effectively a free surface within the plate. Characteristically in tensile fatigue tests it does not initiate immediately next to the first crack. In cyclic bending the system returns to Detail Class C every time the crack reaches a lamination boundary.

The only crack front where propagation might occur in the cleat is the tip of the crack within the depth of the lamination, as seen on the surface. This is a small area on what is probably a blunt crack tip as a result of ductile tearing.

Finally, the angle cleat is constrained to approximately constant curvature in bending over the height of the fillet. The pre-existing ductile crack reduces the effective thickness, but the stresses are also reduced by the curvature compatibility over the height of the cleat, the bending moment finding a path where the full thickness is present.

11. Conclusions

The acoustic emission monitoring of the laboratory test of the angle cleat indicated that no fatigue cracking was initiated or growing with stress ranges up to 175 MPa at the fillet.

The maximum actual measured stress range in an angle cleat of 59.2 MPa (estimated from strain readings) is less than the most conservative Code specification of the Constant Amplitude Fatigue Limit, even with a 31% increase through unforeseen factors.

For all the areas investigated, main girders, cross girders, cleats and gussets, there is no evidence anywhere of fatigue damage, and computations and application of the laboratory and field test results indicate that there should not be any such damage. There is no risk of sudden fatigue failure at all. Normal routine inspection for damage and cracks is all that is required to maintain structural integrity.